FAST TRACK COMMUNICATION • OPEN ACCESS

Fractional Brownian motion in a finite interval: correlations effect depletion or accretion zones of particles near boundaries

To cite this article: T Guggenberger *et al* 2019 *New J. Phys.* **21** 022002

View the article online for updates and enhancements.

New Journal of Physics

The open access journal at the forefront of physics

FAST TRACK COMMUNICATION

Fractional Brownian motion in a finite interval: correlations effect depletion or accretion zones of particles near boundaries

T Guggenberger[1,2], G Pagnini[2], T Vojta[3] and R Metzler[1]

1   Institute of Physics and Astronomy, University of Potsdam, D-14476 Potsdam-Golm, Germany
2   BCAM—Basque Centre for Applied Mathematics, 48009 Bilbao, Basque Country, Spain and Ikerbasque—Basque Foundation for Science, E-48013 Bilbao, Basque Country, Spain
3   Department of Physics, Missouri University of Science and Technology, Rolla, MO 65409, United States of America

E-mail: rmetzler@uni-potsdam.de

Abstract

Fractional Brownian motion (FBM) is a Gaussian stochastic process with stationary, long-time correlated increments and is frequently used to model anomalous diffusion processes. We study numerically FBM confined to a finite interval with reflecting boundary conditions. The probability density function of this reflected FBM at long times converges to a stationary distribution showing distinct deviations from the fully flat distribution of amplitude $1/L$ in an interval of length L found for reflected normal Brownian motion. While for superdiffusion, corresponding to a mean squared displacement (MSD) $\langle X^2(t) \rangle \simeq t^\alpha$ with $1 < \alpha < 2$, the probability density function is lowered in the centre of the interval and rises towards the boundaries, for subdiffusion ($0 < \alpha < 1$) this behaviour is reversed and the particle density is depleted close to the boundaries. The MSD in these cases at long times converges to a stationary value, which is, remarkably, monotonically increasing with the anomalous diffusion exponent α. Our *a priori* surprising results may have interesting consequences for the application of FBM for processes such as molecule or tracer diffusion in the confines of living biological cells or organelles, or other viscoelastic environments such as dense liquids in microfluidic chambers.

1. Introduction

Diffusive transport is quite ubiquitous, ranging from quantum processes such as laser cooling over thermally activated transport in living biological cells, to the dispersal of tracer chemicals in geophysical aquifers. While theoretical works on diffusion often consider infinite or semi-infinite domains, in many cases the particle motion is restricted to a finite interval. Such a scenario is relevant, inter alia, for the dispersal of light in disordered optical cavities, for the motion of thermally driven particles in confining microfluidic chambers, gels, or for the molecular and (sub)micron tracer motion in the confines of biological cells or their organelles. For normal Brownian diffusion in an interval of length L the probability density to find the particle anywhere within this interval has the constant amplitude $1/L$ at sufficiently long times: in the stationary state the particle can be found everywhere equally likely. This property is so engrained in our intuition for random processes that we typically would not question its validity. Indeed, even for generalised random processes such as the continuous time random walk, such equidistributions naturally occur [1–4]. We here show that for the widely used, Gaussian process of fractional Brownian motion (FBM) describing overdamped viscoelastic diffusion, this property is strikingly violated: the inherent negative or positive correlations of FBM in a finite interval effect a pronounced depletion or accretion of the probability density in the vicinity of the boundaries, respectively[4].

---

4 We use the antonyms 'deplete' and 'accrete' in the sense that the system studied here eventually reaches a stationary state with given depletion or accretion zones.

While normal diffusion is characterised by the linear time dependence $\langle X^2(t) \rangle \propto t$ of the mean squared displacement (MSD)[5], *anomalous diffusion* typically classifies the power law time dependence

$$\langle X^2(t) \rangle = 2K_\alpha t^\alpha, \tag{1}$$

of the MSD, where the generalised diffusion coefficient K_α has physical dimension of length^2/time$^\alpha$, and α is the anomalous diffusion exponent. Depending on the value of α one distinguishes between subdiffusion ($0 < \alpha < 1$) and superdiffusion ($\alpha > 1$) [2, 4].

Anomalous diffusion has been observed experimentally and numerically in a wide array of systems [2, 4]. Thus, experimentally subdiffusion is frequently observed for passive particle motion inside living biological cells [5–11] and in crowded, viscoelastic solutions [6, 12–14]. It was also reported from supercomputing studies of lipid and protein molecule motion in bilayer membranes [15–18]. Subdiffusion moreover occurs in other systems, such as for charge carrier motion in amorphous semiconductors [1] or chemical tracers in underground aquifers [19]. Superdiffusion has been observed for the motion of molecular motor-transported particles inside biological cells [20–22], the motion of tracers in two-dimensional rotating flows [23], and for bulk-mediated surface diffusion at liquid–solid interfaces [24].

Normal Brownian motion is characterised by the universal Gaussian probability density [2]. Anomalous diffusion processes lose this universality, and the various possibilities to break the attraction of the basin of the central limit theorem give rise to different mathematical models [25]. For instance, the existence of power-law sojourn times between motion events with a diverging mean waiting time, as indeed measured in single particle tracking experiment [10, 12], lead to anomalous diffusion (1) in the continuous time random walk model [1, 2, 4, 25]. The second very prominent anomalous stochastic process is FBM, first introduced by Kolmogorov [26] and later studied by Mandelbrot and van Ness [27]. FBM is a self-similar, Gaussian process with stationary, long-time correlated increments to describe anomalous diffusion of the power law type (1) in the sub- and superdiffusive range $0 < \alpha < 2$, see below. FBM has been identified as the governing type of motion, or an important ingredient of the motion, for the subdiffusion of various tracers in complex environments both *in vivo* and *in vitro* [9, 11, 14–16, 28], but also for completely different stochastic processes such as electronic network traffic [29] or financial time series [30, 31]. In the superdiffusive regime with $1 < \alpha \leqslant 2$ positive increment correlations and single trajectory power-spectra consistent with FBM were observed for the actively driven motion of endogenous granules inside amoeba cells as well as for the motion of the amoeba themselves [21, 32].

Concurrent to its wide use in diverse fields FBM has been studied in mathematical literature quite extensively, see, for instance, [31, 33, 34]. Nevertheless, many of its fundamental properties remain elusive, especially in the presence of non-trivial boundary conditions. Thus, the method of images[6] typically applied for Brownian motion or random walks with long-tailed waiting time distributions [35] fails and there is no known generalised diffusion equation for FBM that could be solved with direct methods for a given set of boundary values. Among the few results known are the (asymptotic) density of first passage times of FBM confined in a semi-infinite domain [36, 37] and conjectures for a wedge domain [38], as well as the probability density of FBM confined in a semi-infinite interval with an absorbing boundary at the origin in a first order perturbation theory approach [39] [7]. The approach of choice to study FBM in the presence of boundary conditions in most cases is therefore by simulations. We mention that while FBM is asymptotically ergodic, that is, the time average of its MSD in the long time limit converges to the ensemble limit [40], it is transiently ageing [41] and non-ergodic in an external confinement [14, 42]. We finally note that FBM is the basis for a class of stochastic processes called generalised grey Brownian motion [43], which was used to model anomalous diffusion in biological systems [44].

Motivated by a recent study of FBM in a semi-infinite interval with a reflecting boundary at the origin [46], we here investigate by extensive simulations FBM confined to a finite interval with reflecting boundary conditions. The central result is that the naively expected constant amplitude $1/L$ in an interval of length L in the stationary limit for Brownian motion is replaced by a solution for FBM in which the amplitude closer to the boundaries is decreased or increased for subdiffusive and superdiffusive FBM. We analyse this reflected FBM in terms of the probability density function and the MSD. In section 2 we briefly introduce FBM (section 2.1) and

---

[5] Here we restrict our discussion to the one-dimensional process $X(t)$ with initial value $X(0) = 0$. In higher dimensions the motion along different coordinates is viewed as independent.

[6] Similar to the images method in electrodynamics a reflecting or absorbing boundary condition at $x = 0$ for Brownian motion with initial position $x_0 > 0$ can be taken into account by placing a second, imaginary particle (the 'image') at the reflected point $-x_0$ and then summing up (reflecting boundary) or subtracting (absorbing boundary) the respective Green's functions $P(x, t)$ with $P(x, 0) = \delta(x)$, such that the full solution of the boundary value problem is $Q(x, t) = P(x - x_0, t) \pm P(x + x_0, t)$ [35].

[7] We note that FBM should not be confused with scaled Brownian motion (SBM) defined in terms of a diffusion equation with a power-law time dependent diffusivity $D(t) \simeq t^{\alpha-1}$ with $0 < \alpha < 2$ [45]. SBM is Markovian and its probability density function obeys a generalised diffusion equation that can be solved for given boundary conditions.

discuss the implementation of reflecting boundary conditions leading to reflected FBM (section 2.2). In section 3 we present and discuss our results. We present our Conclusions and an outlook in section 4. A comparison of our results for an alternative implementation of reflecting boundary conditions is given in the appendix.

2. A primer on FBM and its numerical implementation

2.1. Fractional Brownian motion

FBM is a centred Gaussian process with covariance function

$$\langle X(t_1)X(t_2) \rangle = K_\alpha(t_1^\alpha + t_2^\alpha - |t_1 - t_2|^\alpha) \tag{2}$$

and continuous sample paths defined for anomalous diffusion exponents in the interval $0 < \alpha < 2$ [31]. For $\alpha = 1$ FBM is a Wiener process describing Brownian motion. From definition (2) it follows that FBM starts at the origin, $X(0) = 0$, has the MSD (1), and the free-space Gaussian probability density function

$$P(x, t) = \frac{1}{\sqrt{4\pi K_\alpha t^\alpha}} \exp\left(-\frac{x^2}{4K_\alpha t^\alpha}\right). \tag{3}$$

Furthermore, the increments of FBM are stationary but—except for the case of Brownian motion ($\alpha = 1$)—long-time correlated and hence not independent. For superdiffusion ($\alpha > 1$) and subdiffusion ($\alpha < 1$), respectively, the increments are positively and negatively correlated [31], see below. These correlations are the cause for the strongly non-Markovian nature of FBM and the lack of a complete mathematical apparatus to analytically deal with the process in the presence of a fixed length (and, by virtue of the MSD, thus time) scale. FBM is a self-similar process with parameter $\alpha/2$: for all $c > 0$, in distribution $X(ct) = c^{\alpha/2}X(t)$. This means that the paths of FBM are time scale-invariant up to a constant factor, that is, they statistically appear the same in rescaled time intervals.

Despite the deceivingly simple form of the probability density function (3), naively employing the method of images to construct the first passage time density leads to erroneous results [37, 38, 47][8]. Passing over to a discrete time version of FBM that can be implemented numerically, we here define reflected FBM as follows. Discrete time FBM is taken as $Y_n = X(\epsilon n)$, where $\epsilon > 0$ is a time step. Its increment process $R_n = Y_{n+1} - Y_n$ is discrete time fractional Gaussian noise (FGN). From this definition it follows that discrete FGN is a stationary, centred Gaussian process with covariance

$$\langle R_i R_{i+j} \rangle = K_\alpha \epsilon^\alpha(|j + 1|^\alpha + |j - 1|^\alpha - 2 |j|^\alpha). \tag{4}$$

The random variables defined by FGN are thus identically Gaussian-distributed, but, except for the case of Brownian motion with $\alpha = 1$, long time correlated and hence not independent, such that the emerging process FBM is strongly non-Markovian. For superdiffusion (subdiffusion) the increments are positively (negatively) correlated

$$\langle R_i R_{i+j} \rangle \begin{cases} >0, & \alpha > 1 \\ =0, & \alpha = 1. \\ <0, & \alpha < 1 \end{cases} \tag{5}$$

In the long-time limit $j \to \infty$ the correlations tend to zero, the asymptotic form reading $\langle R_i R_{i+j} \rangle \sim K_\alpha \epsilon^\alpha \alpha(\alpha - 1)j^{\alpha-2}$.

Using the definition of discrete time FGN, discrete time FBM satisfies the recursion relation

$$Y_0 = 0, \quad Y_{n+1} = Y_n + R_n \tag{6}$$

with the solution

$$Y_n = \sum_{i=0}^{n-1} R_i. \tag{7}$$

Discrete time FBM can thus be considered as a random walk with identically Gaussian distributed but long-time correlated steps. By simulating discrete time FGN and using the recursion relation (6), discrete time FBM can be directly obtained.

---

[8] Expression (3) is in fact identical with the probability density function of scaled Brownian motion in unbounded space for which the generalised diffusion equation is known and Markovian. Using the method of images based on solution (3) to determine the survival of a particle for an absorbing boundary is consistent with the first passage behaviour of scaled Brownian motion.

2.2. Reflected FBM

To implement the reflecting boundary condition and thus define discrete time reflected FBM Z_n we use discrete time FGN and modify the recursion relation (6) appropriately. On the semi-infinite interval $[0, \infty)$ we define reflected FBM by

$$Z_0 = 0,$$
$$Z_{n+1} = |Z_n + R_n|. \tag{8}$$

This means that if the particle attempts to jump across the boundary of the interval by a distance $d > 0$ to the left, that is, attempts to perform the move $0 \leqslant Z_n \to Z_n + R_n = -d < 0$, it is instead reflected and placed inside the interval with the same distance to the boundary. While definition (8) is local in space and identical to the one used for normal Brownian motion, due to the built-in correlations of FGN, the probability density function of reflected FBM does not possess a horizontal derivative at the boundary for $\alpha \neq 1$, as was reported in [46]. The standard horizontal-derivative boundary condition for a reflecting boundary is thus not valid for FBM, which is intimately connected with the above statement that the method of images cannot be applied.

The definition of the recursion relation for discrete time reflected FBM in a *finite* interval $[a, b]$ $(a < 0 < b)$ is based on the same idea for either of the two boundaries. However, for a finite interval one has to consider the possibility that the particle jumps across the boundary by a distance greater than the interval length $L = b - a$, that is, $d > L$. Then, simply reflecting the particle as for the semi-infinite interval would place it outside the interval. While in our simulations below the interval length L is much larger than the average single jump length and thus such effects essentially never occur, to fully rule out this possibility the particle is kept reflecting alternately at both boundaries until it is finally reflected into (placed inside) the interval. This procedure indeed works for any L and d and leads to the recursion relation (A.1). Our study here demonstrates that even in the stationary limit for $n \to \infty$ the probability density function is not given by the constant value $1/L$, apart from the normal Brownian case without correlations. Instead the value of the probability density is significantly depleted or accreted for sub- and superdiffusion. This phenomenon will effect non-negligible consequences on natural systems in which tracer particles follow the laws of FBM, as we discuss in section 4.
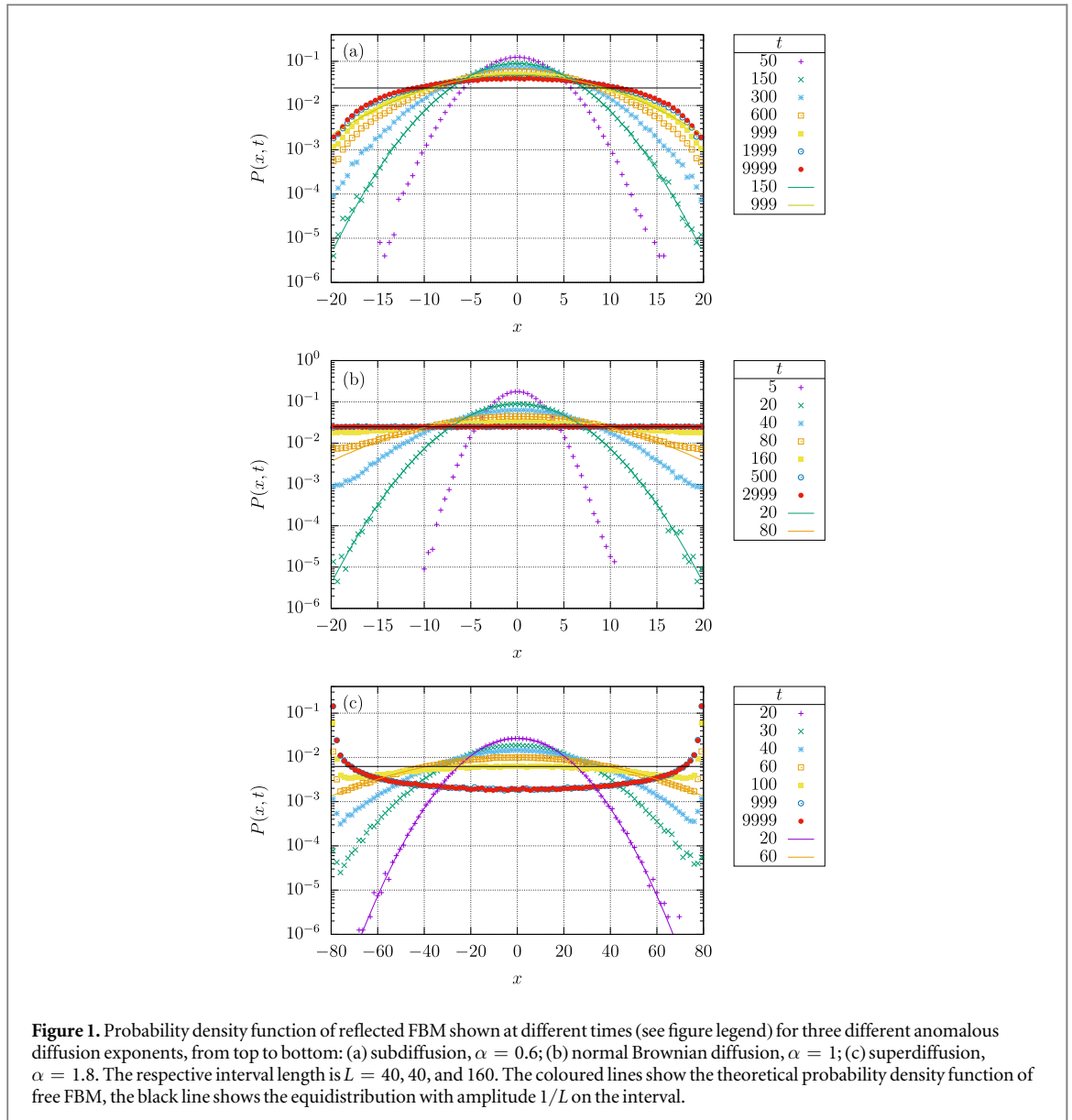
Note that reflected FBM could, in principle, also be defined differently. In appendix A we demonstrate that this alternative choice does not lead to the same behaviour and already produces inconsistent results for normal Brownian diffusion. In the following we employ the meaningful definition of reflected FBM given in equation (8).

3. Probability density function and MSD of reflected FBM

For the simulation of discrete time FGN we employed the Cholesky method [48], which can be used to simulate an arbitrary Gaussian process, given its expectation and covariance function. As underlying random number generator we used the Saito and Matsumoto SIMT-oriented Fast Mersenne Twister. The anomalous diffusion coefficient was set to $K_\alpha = 1/2$ in units of cm^2/s$^\alpha$ and the anomalous diffusion exponent α ranged from 0.5 to 1.8. We used a symmetric interval $[-L/2, L/2]$ centred at the origin, and the interval length L was changed from 10 to 2000 in units of cm. The time step was set to $\epsilon = 1$ in units of s, and we performed simulations with up to $N = 2 \times 10^4$ time steps and $M = 5 \times 10^5$ trajectories, chosen such as to guarantee sufficient convergence of the results. In all runs the initial condition placed the particle at the origin, $X_0 = 0$. In the following all quantities corresponding to unconfined FBM are called 'free'.

3.1. Probability density function

Figure 1 shows the probability density function of reflected FBM for three different anomalous diffusion exponents. We make the following observations. (i) At all times the shape of the probability density is symmetric with respect to the origin, $P(-x, t) = P(x, t)$, consistent with the symmetric definition of the process. (ii) At sufficiently short times the probability density coincides with that of the corresponding free FBM, equation (3), as it should be. (iii) At longer times the effect of the boundary becomes significant and the probability density deviates from that of free FBM. We note that even in the superdiffusive case in figure 1(c) the solution of free FBM still shows very good agreement with reflected FBM at intermediate times, apart from the region close to the boundaries, demonstrating a relatively slow propagation of the boundary-effected disturbance of the probability density. In the limit of very long times the probability density function converges to a stationary limit. (iv) Strikingly, while for normal Brownian diffusion the stationary form of the probability density has the constant amplitude $1/L$, for sub- and superdiffusion the stationary shape deviates significantly from this equidistribution. Namely, compared to the $1/L$-equidistribution, for subdiffusion the stationary probability density is increased in the central region of the interval and monotonically decreases towards the boundary, attaining amplitudes significantly below $1/L$ over an appreciable boundary zone. In contrast, for superdiffusion the stationary probability density is decreased in the central region of the interval and monotonically increases

Figure 1. Probability density function of reflected FBM shown at different times (see figure legend) for three different anomalous diffusion exponents, from top to bottom: (a) subdiffusion, $\alpha = 0.6$; (b) normal Brownian diffusion, $\alpha = 1$; (c) superdiffusion, $\alpha = 1.8$. The respective interval length is $L = 40$, 40, and 160. The coloured lines show the theoretical probability density function of free FBM, the black line shows the equidistribution with amplitude $1/L$ on the interval.
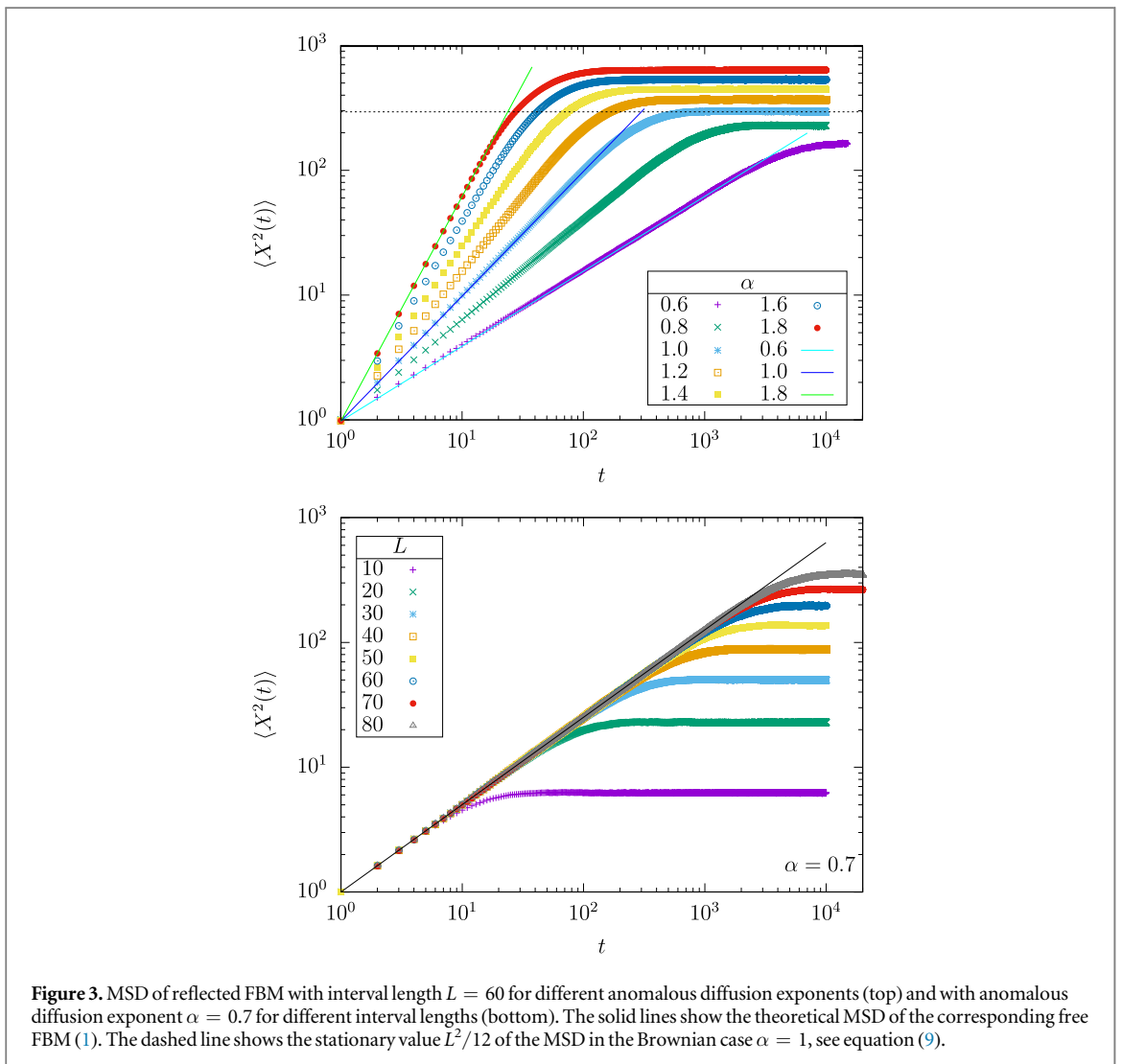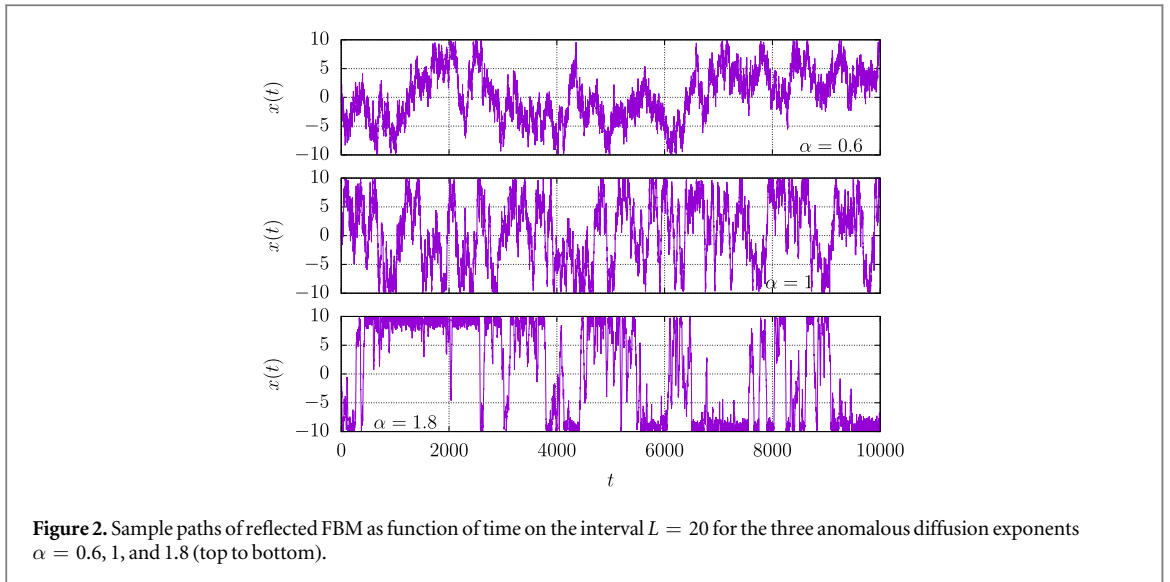
towards the boundary. Moreover, for superdiffusion at intermediate times the behaviour of the probability density is non-monotonic between the origin and the boundary.

The behaviour of the probability density of reflected FBM can be explained qualitatively as follows. For subdiffusion the jumps R_n that the particle performs are negatively correlated. Therefore, if the particle jumps across the boundary and gets reflected in one step, in the next step it tends to jump to the opposite direction, away from the boundary. Hence, the particle on average tends to stay away from the boundary region and thus the probability density in that region is depleted. For superdiffusion the jumps are positively correlated and therefore, if the particle jumps across the boundary and gets reflected in one step, in the next step it tends to jump in the same direction, towards the boundary. This leads to an accretion of particle probability in the boundary region. For normal Brownian diffusion, in contrast, the jumps are uncorrelated and hence the particle has no tendency to stay in or stay away from the boundary region. This effects the simple equidistribution with amplitude $1/L$. Figure 2 shows a typical sample path for normal Brownian diffusion, sub- and superdiffusion, and nicely illustrates this behaviour.
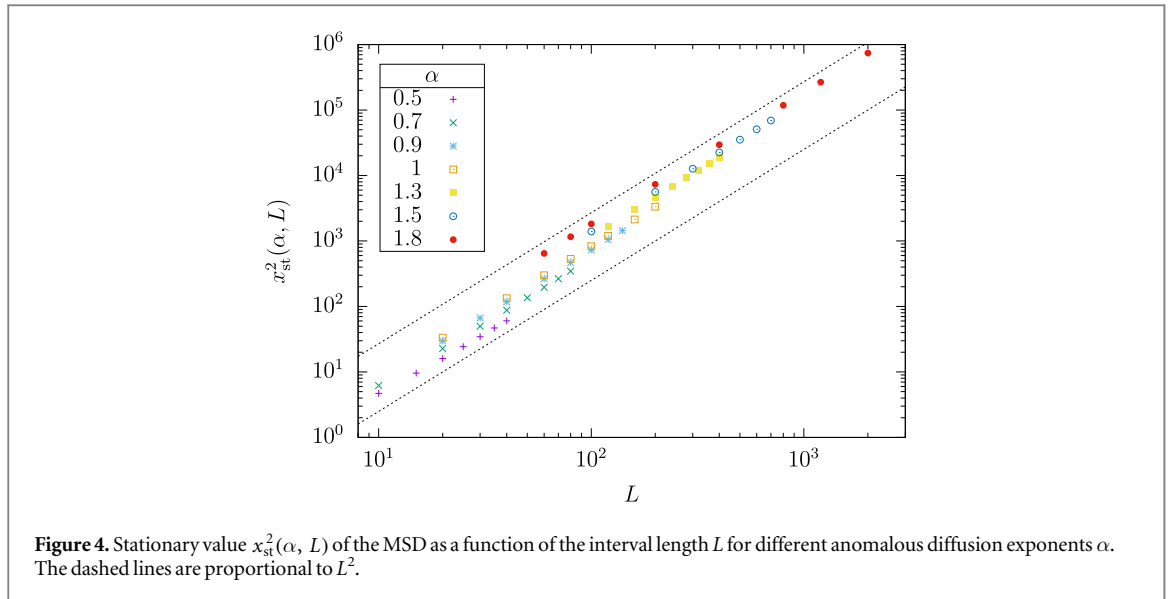
3.2. Mean squared displacement
We now show that the effects observed for the probability density function also translate to the behaviour of the MSD. Figure 3 shows the MSD of reflected FBM with interval length $L = 60$ for different anomalous diffusion exponents (top) and with anomalous diffusion exponent $\alpha = 0.7$ for different interval lengths (bottom). At short times the MSD behaves like that of the corresponding free FBM, as it should. However, at long times the

Figure 2. Sample paths of reflected FBM as function of time on the interval $L = 20$ for the three anomalous diffusion exponents $\alpha = 0.6$, 1, and 1.8 (top to bottom).

Figure 3. MSD of reflected FBM with interval length $L = 60$ for different anomalous diffusion exponents (top) and with anomalous diffusion exponent $\alpha = 0.7$ for different interval lengths (bottom). The solid lines show the theoretical MSD of the corresponding free FBM (1). The dashed line shows the stationary value $L^2/12$ of the MSD in the Brownian case $\alpha = 1$, see equation (9).

MSD converges to the stationary value $x_{st}^2(\alpha, L) = \lim_{t \to \infty} \langle X^2(t) \rangle$, which is monotonically increasing with the anomalous diffusion exponent α and the interval length L. Since in the case of reflected Brownian motion ($\alpha = 1$) the stationary probability density is given by the equidistribution $P_{st}(x) = 1/L$, in that case the stationary value of the MSD simply becomes

Figure 4. Stationary value $x_{st}^2(\alpha, L)$ of the MSD as a function of the interval length L for different anomalous diffusion exponents α. The dashed lines are proportional to L^2.

Table 1. Values of the fit parameters a and b, resulting from fits of the stationary value of the MSD as a function of L for each α. The statistical uncertainties of the fit-parameter values are smaller than 10^{-2}.

α	a	b
0.5	0.05	1.91
0.7	0.06	1.98
0.9	0.07	2.00
1.0	0.08	2.00
1.3	0.11	2.01
1.5	0.14	2.00
1.8	0.18	2.00

$$x_{st}^2(\alpha = 1, L) = \int_{-L/2}^{L/2} \frac{x^2}{L} \mathrm{d}x = \frac{L^2}{12}. \tag{9}$$

This value is shown as dashed line in figure 3.

We determined the MSD of reflected FBM for a range of α values and several interval lengths L for each fixed α (the case $\alpha = 0.7$ is shown in figure 3). From these we determined the stationary values of the MSD as mean values from the stationary plateaus. Figure 4 shows the stationary value of the MSD versus the interval length for the different anomalous diffusion exponents. The dashed lines corroborates that the stationary value of the MSD is proportional to the squared interval length, independent of the anomalous diffusion exponent. We fitted[9] the stationary values of the MSD for each α as a function of L with the fit-function $f(L) = aL^b$ and fit parameters a and b. The resulting values of the fit parameters shown in table 1 nicely corroborate the conjecture of the L^2-proportionality. The slight deviation from the value 2 for the case $\alpha = 0.5$ is likely due to finite size effects, as for this most subdiffusive value the attained value is quite short, and in figure 3 the plateau has not been fully reached.

From the α dependence of the stationary MSD shown in figure B1 for different interval lengths L we deduce that the data are consistent with the functional form $x_{st}^2(\alpha, L) = \alpha^c \times L^2/12$, where $L^2/12$ is its value in the Brownian limit $\alpha = 1$, and $c > 0$.

4. Conclusion

We studied by simulations the stochastic process of reflected FBM, which is confined to a finite interval with reflecting boundary conditions, a situation that is typical for tracer particles in the viscoelastic confines of biological cells or their organelles, as well as in artificially crowded liquids in microfluidic devises and similar. We found that the stationary probability density function of this reflected FBM significantly deviates from the

---

[9] We used the gnuplot fit routine based on the nonlinear least-square Marquardt–Levenberg algorithm.

equidistribution with amplitude $1/L$ found for reflected Brownian motion ($\alpha = 1$). In particular, for superdiffusion ($1 < \alpha < 2$) the stationary probability density is decreased in the centre of the interval and particle accretion occurs towards the boundaries, reaching amplitudes above $1/L$. For subdiffusion ($0 < \alpha < 1$) this behaviour is reversed, and we observe a distinct depletion of the probability density in an appreciable region around the boundaries. The MSD at long times converges to a stationary value, which is monotonically increasing with rising anomalous diffusion exponent $0 < \alpha < 2$ and interval length $L > 0$. Our simulation results corroborate that the stationary value of the MSD is proportional to L^2 for all α.

The form of the stationary probability density function can be qualitatively explained as a result of the interplay between the positive or negative correlations of the discrete time FGN (the steps used to generate reflected FBM) and the boundary conditions. It is tempting to ask to which extent the observed form of the stationary probability density function is universal for centred Gaussian processes with stationary, positively (negatively) long-time correlated increments under confinement with reflecting boundary conditions. In the case of positive correlations, it is conjectured in [46] that for increments asymptotically decaying for large n as $n^{\alpha-2}$ with $1 < \alpha < 2$ the stationary probability density equals that of the corresponding reflected FBM, and for a decay faster than n^{-1} the stationary probability density agrees with that of reflected Brownian motion. For short-time correlations (positive or negative with at least exponentially fast decay) we naturally expect the stationary probability density to agree with that of reflected Brownian motion. A more detailed study of such processes will be of interest. Similarly, it should be analysed how the relaxation behaviour of both the MSD and the probability density function looks like when we introduce hard or soft cutoffs to the FGN, as recently studied in [49]. Finally, it will be interesting to see how corresponding stochastic processes fuelled by FGN but with distributed (superstatistical) diffusivities [50] behave under confinement.

As mentioned above FBM is widely used to model anomalous diffusion in various complex systems, particularly for (sub)micron-sized tracer particles such as vesicles, granules, viruses, or tracer beads in the crowded cytoplasm of biological cells or in artificially crowded liquids. Inside cells, but also in many situations *in vitro*, boundaries in the form of cellular membranes or microfluidic chambers play an essential role. Cognisance of depletion layers around boundaries in the case of passive subdiffusion or accretion layers for actively driven, superdiffusive particles will likely affect model calculations for interactions with the boundaries, for instance, the binding to membrane embedded receptors. It is an interesting question how these boundary effects conspire with other, concurrent effects. Thus, in a microfluidic chamber or inside a simple membrane vesicle, the depletion/accretion effects due to reflected FBM may superimpose with transient sticking to the boundary. This could be studied quantitatively in a reflected FBM model with a sticking time distribution to the reflecting boundary, or in terms of reactive (Robin) boundary conditions. In real biological cells, we could think of even more complicated situations. Thus, many cells have an enriched layer of actin cytoskeleton close to the cell wall. Passive tracer particles may therefore be trapped intermittently in cages [12, 51], countering the depletion effects due to subdiffusive FBM. Both experiments and detailed simulations will be necessary to scrutinise this phenomenon. In this context we may venture a simple scaling argument. The fact that the stationary MSD data show an L^2 dependence with a prefactor different from $1/12$ implies that the extra contribution to the probability density caused by the boundaries is not confined to a finite interval close to the walls, as otherwise a convergence to the value $1/12$ for large L should be observed. Indeed, such a situation would not be surprising if we assume that the behaviour of the probability density is similar to the power-law found for a semi-infinite domain in [46]. We also note that the L^2 proportionality of the stationary MSD puts a constraint on the exact form of the probability density. If we assume naive scaling, at least in the limit $L \gg K_\alpha^{1/2}$ at unit time we would expect a functional behaviour of the stationary probability density of the form $P(x, L) = (1/L)g(x/L)$, where $g(\cdot)$ is a scaling function. Consistent with our arguments, the depletion/accretion zone width thus scales with L and becomes a non-negligible effect. The exact determination of the width of the depletion or accumulation layer as function of L, K_α and α will be the topic of future research.

It is instructive to compare our results for the MSD in our finite interval L with those for FBM confined in an harmonic potential $V(x) = (k/2)x^2$ ($k > 0$) as studied in [42, 47]. The main difference, for any stochastic process, is that the random motion in an interval with reflecting boundaries (infinitely steep confining potential) is athermal, that is, its stationary state does not involve the diffusion coefficient. In a confining potential, processes such as normal Brownian diffusion or continuous time random walks with any distribution of waiting times always converge to the corresponding Boltzmann solution with a well defined temperature [4, 25]. FBM, in contrast to the fractional Langevin equation fulfilling Kubo's fluctuation-dissipation relation [52, 53], converges to a stationary state depending on both the generalised diffusivity K_α and the anomalous diffusion exponent α, a fact that follows from the corresponding (overdamped) Langevin equation fuelled by FGN [42, 47]. At short times the MSD of this process grows like that of unconfined FBM. At long times it converges to the stationary value $x_{\mathrm{st}}^2(k, \alpha) = (K_\alpha/k^\alpha)\Gamma(\alpha + 1)$ in terms of the Γ-function. Its stationary value, in contrast
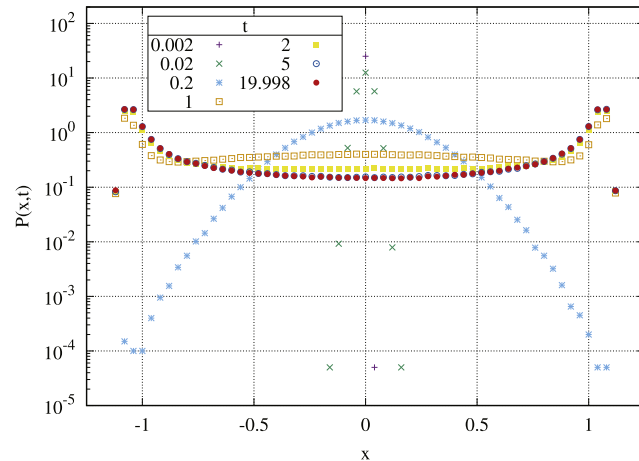
Figure 5. Probability density function of superdiffusive FBM with $\alpha = 1.8$ in the external potential $V_{16}(x) = x^{32}/160$ for varying times. Similar to reflected FBM, accretion zones emerge in the wings of the stationary distribution.
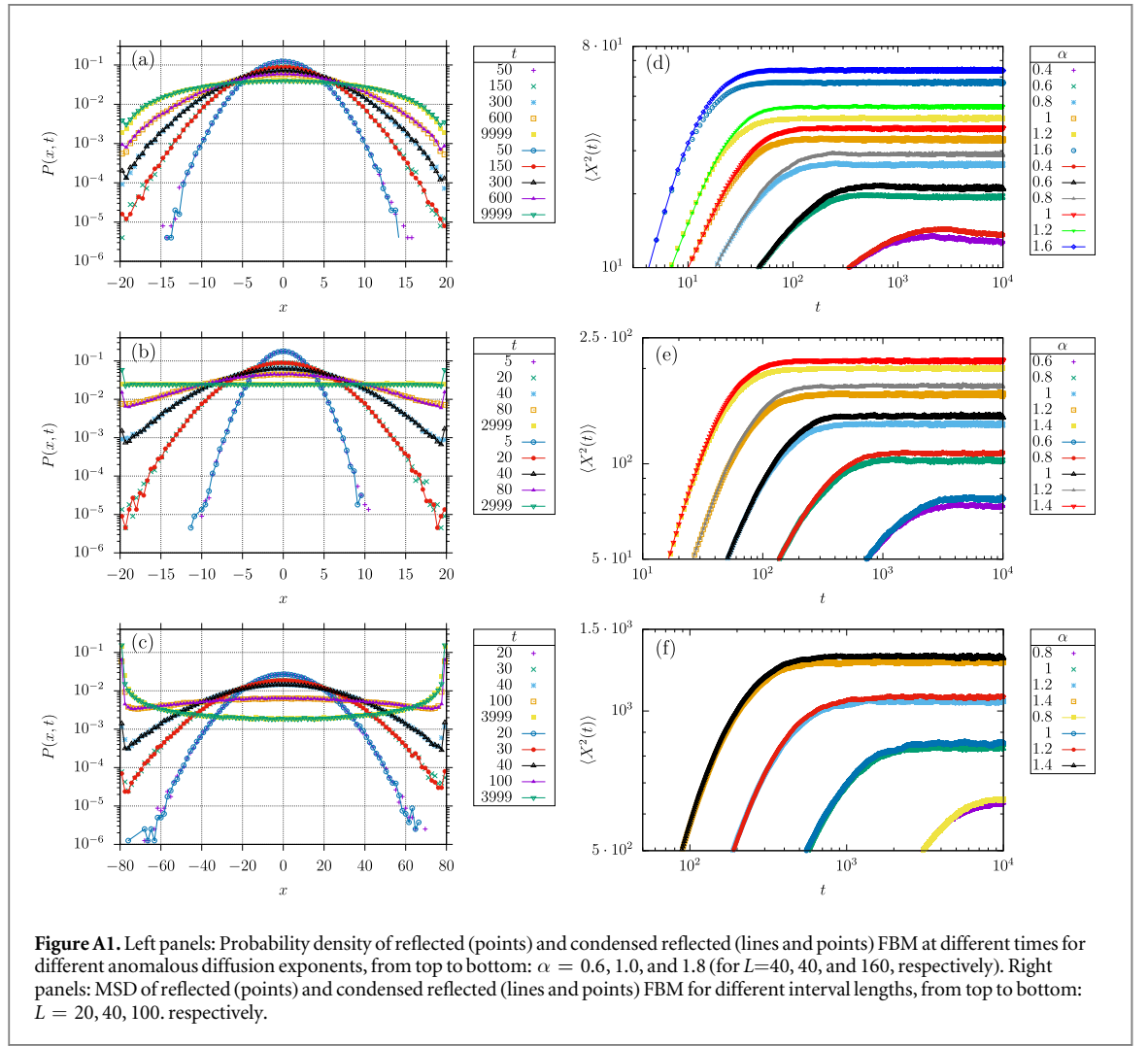
to the strictly monotonic dependence on α of x_{st}^2 for reflected FBM, is in general a non-monotonic function of α [47]. Moreover, it can be shown that the transition of the MSD to the stationary value is exponential with the single characteristic time scale $1/k$, such that stationarity is reached at a time independent of α [42]. In contrast, for reflected FBM the time at which stationarity is reached strongly depends on α, as evidenced by figure 3 (top). Hence, the MSD of reflected FBM behaves fundamentally different from that of FBM confined to move in an harmonic potential. We expect that this fundamental differences between reflected and potential-confined FBM persists when the harmonic potential is generalised to steeper potential $V_n(x) = kx^{2n}/(2n)$ with $n > 2$. However, what happens in the limit $n \to \infty$? In this case, the potential essentially describes a potential well in $[-1, 1]$ with infinitely high walls. Hence, the particles can move freely inside that region, but are still confined to it (by the infinitely high potential walls), similar to the case with reflecting boundary conditions. This argument is indeed corroborated by the data in figure 5. It remains open exactly for which n such a crossover can be observed and what the associated relaxation dynamics is.

The case of an ever steeper external potential may also be used as an argument in favour of the approach chosen herein with respect to the FGN driving the reflected FBM process. Namely, we once create a time series of noise increments that we use as input in our simulations, upon reflection at one of the two walls the FGN time series is simply continued. One may ask whether the memory of the FGN due to the built-in power-law correlations should not be reset once a reflection event occurs. No such complication is expected when we consider FBM in a moderate external potential, for instance, the above-mentioned harmonic potential. Here the action of the potential is taken to superimpose to the FGN, consistent with the quantative modelling of experiments [14]. If we now make the external potential much steeper, we would expect that the argument of un-interrupted FGN still holds. However, as we demonstrate in figure 5 for the superdiffusive case already in this case significant accretion zones are created[10]. The ultimate answer whether the approach with invariant FGN is justified in systems such as biological cells will, of course, have to come from experiments.

Acknowledgements

---

[10] Note that this effect is similar to the emergence of multimodal distributions for strongly confined Lévy flights [54].

Figure A1. Left panels: Probability density of reflected (points) and condensed reflected (lines and points) FBM at different times for different anomalous diffusion exponents, from top to bottom: $\alpha = 0.6$, 1.0, and 1.8 (for $L=40$, 40, and 160, respectively). Right panels: MSD of reflected (points) and condensed reflected (lines and points) FBM for different interval lengths, from top to bottom: $L = 20, 40, 100$. respectively.

Appendix A. Alternative boundary conditions produce inconsistent results

Based on the procedure of alternate reflections described in section 2.2 one arrives at a recursion relation for discrete time reflected FBM in a finite interval by the following argument. Denote with $D_n = \min\{|Z_n + R_n - a|,$ $|Z_n + R_n - b|\}$ the distance of the particle to the nearest boundary after its $(n + 1)$th jump. If this leads the particle across a boundary (for instance, $Z_n + R_n > b$), D_n is the distance of the particle to this boundary. Then $S_n = D_n \bmod L$ is the jump length of the last reflection, by which the particle is finally placed inside the interval. If the interval length L 'fits into' the distance D_n evenly ($\lfloor D_n/L \rfloor$ even) the last reflecting boundary is equal to the one jumped across first[11]. If $\lfloor D_n/L \rfloor$ is odd, the last reflecting boundary is opposite to the one jumped across first. Hence, we define discrete time reflected FBM in the finite interval $[a, b]$ by $Z_0 = 0$ and

$$Z_{n+1} = \begin{cases} Z_n + R_n, & a \leqslant Z_n + R_n \leqslant b \\ b - S_n, & Z_n + R_n > b \text{ and } \lfloor D_n/L \rfloor \text{even or} \\ & Z_n + R_n < a \text{ and } \lfloor D_n/L \rfloor \text{odd} \\ a + S_n, & Z_n + R_n > b \text{ and } \lfloor D_n/L \rfloor \text{odd or} \\ & Z_n + R_n < a \text{ and } \lfloor D_n/L \rfloor \text{even.} \end{cases} \tag{A.1}$$

One can easily think of other boundary conditions which can justifiably be called 'reflecting' and which thus lead to corresponding 'reflected' FBM. A particular simple choice is defined such that if the particle jumps across the boundary, it is placed exactly on this boundary. We call this a 'condensed reflecting boundary condition'. Hence, the corresponding condensed reflected FBM in the interval $[a, b]$ is defined by $Z_0 = 0$ and

[11] The symbol $\lfloor \cdot \rfloor$ denotes the floor function. For any real number x, $\lfloor x \rfloor$ is the largest integer less than or equal to x: $\lfloor x \rfloor = \max_{n \in \mathbb{Z}}$ for $n \leqslant x$.
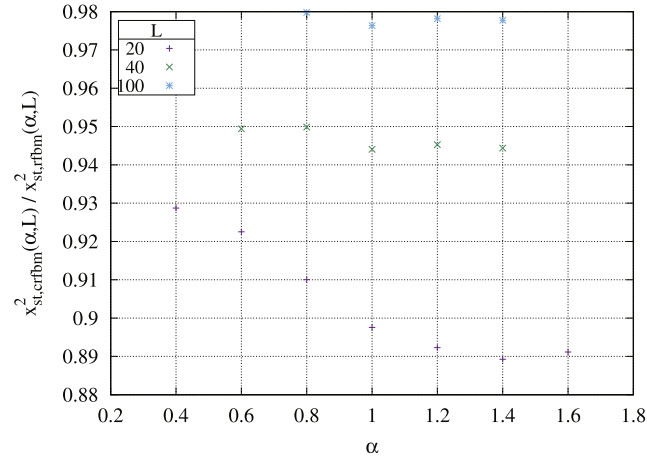
Figure A2. Ratio of the stationary MSDs for condensed reflected FBM and reflected FBM as function of α, and for three different interval lengths L.

$$Z_{n+1} = \begin{cases} Z_n + R_n, & a \leqslant Z_n + R_n \leqslant b \\ a, & Z_n + R_n < a \\ b, & Z_n + R_n > b \end{cases} \qquad (A.2)$$

In this appendix we compare our simulation results for reflected FBM defined by (A.1) shown in the main text with results for condensed reflected FBM (A.2).

In the left panels of figure A1 we show the probability density of reflected and condensed reflected FBM for different anomalous diffusion exponents. At short times the behaviour for both boundary conditions coincide. This is due to the fact that boundary effects become significant only at longer times, when a significant portion of particles had enough time to reach the boundary. At longer times the probability density of condensed reflected FBM shows a distinct cusp at the boundary, where the values of the probability density are larger than those for reflected FBM. This cusp persists also in the stationary distribution, and is present for normal Brownian diffusion, as well. The cusp naturally stems from the 'condensation' of all reflected particles right at the position of the wall. Clearly, this boundary condition is not consistent with the known results for Brownian diffusion, and we therefore discard this alternative definition. To complement this claim, in the right panels of figure A1 we show the MSD of reflected and condensed reflected FBM for different interval lengths. At short times the MSD for both boundary conditions coincide. At longer times they deviate, the stationary value for condensed reflected FBM being larger than that for reflected FBM. This is due to the fact that the condensed particles at the boundaries contribute to the MSD with a higher amplitude than the distributed reflected particles in the proper reflected FBM process. Of course, the deviations due to the exact choice of how to implement reflecting boundary conditions is expected to become increasingly less relevant when the size L of the interval becomes larger, $L \gg K_\alpha^{1/2}$ at unit time.

Figure A2 shows the ratio $x_{\text{st,crfbm}}^2(\alpha, L)/x_{\text{st,rfbm}}^2(\alpha, L)$ of the stationary MSDs for condensed reflected FBM and reflected FBM. For the largest interval length, $L = 100$, the ratio becomes practically unity, demonstrating that the definition of the reflecting boundary condition only disturbs a finite zone around the boundaries.

Appendix B. Stationary MSD versus α

Figure B1 shows the dependence of the stationary MSD $x_{\text{st}}^2(\alpha, L)$ on the anomalous diffusion exponent α. The dashed lines show a linear fit while the full lines represent fits to the quadratic form $g(\alpha, L) = a\alpha^c \times L^2/12$ with the fit parameters a and c listed in table B1. The fact that $a \approx 1$ in all cases corroborates the $L^2/12$-prefactor in the functional form $x_{\text{st}}^2(\alpha, L) = \alpha^c \times L^2/12$, while c clearly increases with α.

Figure B1. Stationary MSD x_{st}^2 as function of α. See text for details.
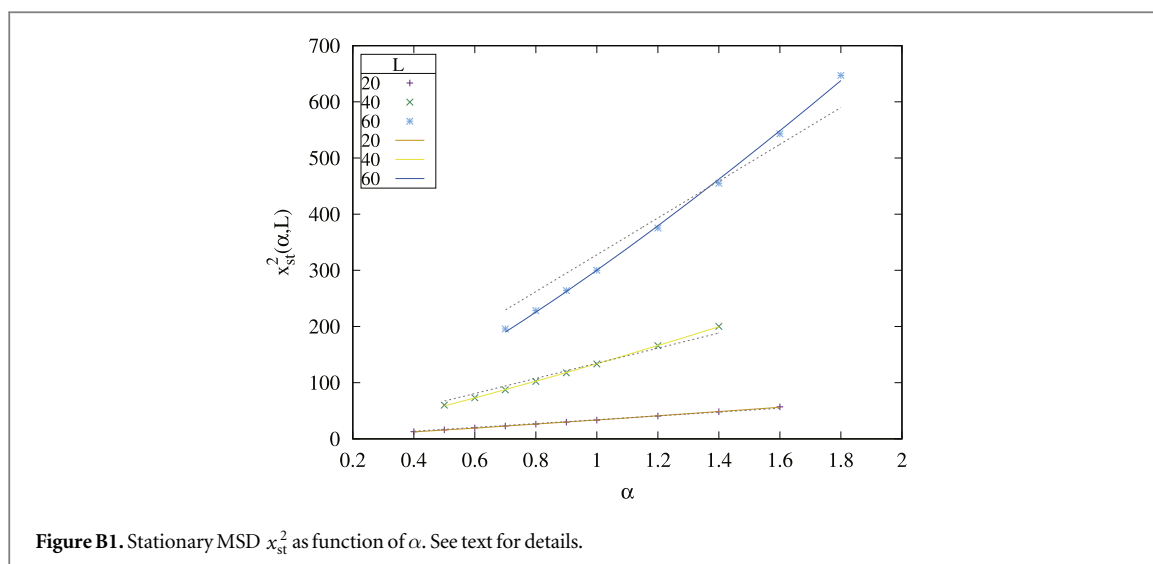
Table B1. Fit parameters for the data of figure B1.

L	a	c
20	1.01	1.10
40	1.00	1.19
60	1.00	1.28

ORCID iDs

R Metzler ⓘ https://orcid.org/0000-0002-6013-7020

References

[1] Scher H and Montroll E W 1975 *Phys. Rev.* B **12** 2455
[2] Bouchaud J-P and Georges A 1990 *Phys. Rep.* **195** 127
[3] Metzler R and Klafter J 2000 *Physica* A **278** 107
[4] Metzler R and Klafter J 2000 *Phys. Rep.* **339** 1
[5] Höfling F and Franosch T 2013 *Rep. Prog. Phys.* **76** 046602
      Nørregaard K, Metzler R, Ritter C M, Berg-Sørensen K and Oddershede L B 2017 *Chem. Rev.* **117** 4342
[6] Weiss M, Elsner M, Kartberg F and Nilsson T 2004 *Biophys. J.* **87** 3518
[7] Golding I and Cox E C 2006 *Phys. Rev. Lett.* **96** 098102
[8] Bronstein I, Israel Y, Kepten E, Mai S, Shav-Tal Y, Barkai E and Garini Y 2009 *Phys. Rev. Lett.* **103** 018102
      Burnecki K, Kepten E, Janczura J, Bronshtein I, Garini Y and Weron A 2012 *Biophys. J.* **103** 1839
[9] Weber S C, Spakowitz A J and Theriot J A 2010 *Phys. Rev. Lett.* **104** 238102
      Jeon J-H, Tejedor V, Burov S, Barkai E, Selhuber-Unkel C, Berg-Sørensen K, Oddershede L and Metzler R 2011 *Phys. Rev. Lett.* **106** 048103
[10] Weigel A V, Simon B, Tamkun M M and Krapf D 2011 *Proc. Natl Acad. Sci. USA* **108** 6438
      Weigel A V, Tamkun M M and Krapf D 2013 *Proc. Natl Acad. Sci. USA* **110** E4591
[11] Tabei S M, Burov S, Kim H Y, Kuznetsov A, Huynh T, Jureller J, Philipson L H, Dinner A R and Scherer N F 2013 *Proc. Natl. Acad Sci. USA* **110** 4911
[12] Wong I Y, Gardel M L, Reichman D R, Weeks E R, Valentine M T, Bausch A R and Weitz D A 2004 *Phys. Rev. Lett.* **92** 178101
[13] Banks D S and Fradin C 2005 *Biophys. J.* **89** 2960
      Pan W, Filobelo L, Pham N D Q, Galkin O, Uzunova V V and Vekilov P G 2009 *Phys. Rev. Lett.* **102** 058101
[14] Jeon J-H, Leijnse N, Oddershede L B and Metzler R 2013 *New J. Phys.* **15** 045011
[15] Jeon J-H, Monne H M-S, Javanainen M and Metzler R 2012 *Phys. Rev. Lett.* **109** 188103
[16] Kneller G R, Baczynski K and Pasenkiewicz-Gierula M 2011 *J. Chem. Phys.* **135** 141105
[17] Gupta S, de Mel J U, Perera R M, Zolnierczuk P, Bleuel M, Faraone A and Schneider G J 2018 *J. Phys. Chem. Lett.* **9** 2956
      He W, Song H, Su Y, Geng L, Ackerson B J, Peng H B and Tong P 2016 *Nat. Comm.* **7** 11701
[18] Jeon J-H, Javanainen M, Martinez-Seara H, Metzler R and Vattulainen I 2016 *Phys. Rev. X* **6** 021006
[19] Ederi Y, Guadagnini A, Scher H and Berkowitz B 2014 *Water Res. Res.* **50** 1490
[20] Caspi A, Granek R and Elbaum M 2002 *Phys. Rev. E* **66** 011916
[21] Reverey J F, Jeon J-H, Bao H, Leippe M, Metzler R and Selhuber-Unkel C 2015 *Sci. Rep.* **5** 11690
[22] Song M, Moon H C, Jeon J-H and Park H Y 2018 *Nat. Commun.* **9** 344
      Chen K J, Wang B and Granick S 2015 *Nat. Mater.* **14** 589
[23] Solomon T H, Weeks E R and Swinney H L 1993 *Phys. Rev. Lett.* **71** 3975

[24] Krapf D, Campagnola G, Nepal K and Peersen O B 2016 *Phys. Chem. Chem. Phys.* **18** 12633
     Skaug M J, Mabry J and Schwartz D K 2013 *Phys. Rev. Lett.* **110** 256101
     Chechkin A V, Zaid I M, Lomholt M A, Sokolov I M and Metzler R 2012 *Phys. Rev.* E **86** 041101
[25] Metzler R, Jeon J-H, Cherstvy A G and Barkai E 2014 *Phys. Chem. Chem. Phys.* **16** 24128
[26] Kolmogorov A N 1940 *Dokl. Akad. Nauk SSSR* **26** 115
[27] Mandelbrot B B and van Ness J W 1968 *SIAM Rev.* **10** 422
[28] Guigas G and Weiss M 2008 *Biophys. J.* **94** 90
     Magdziarz M, Weron A, Burnecki K and Klafter J 2009 *Phys. Rev. Lett.* **103** 180602
     Szymanski J and Weiss M 2009 *Phys. Rev. Lett.* **103** 038102
[29] Mikosch T, Resnick S, Rootzén H and Stegeman A 2002 *Ann. Appl. Probab.* **12** 23
[30] Comte F and Renault E 1998 *Math. Financ.* **8** 291
     Rosteck S and Schöbel R 2013 *Econ. Modelling* **30** 30
[31] Biagini F, Hu Y, Øksendal B and Zhang T 2008 *Stochastic Calculus for Fractional Brownian Motion and Applications* (Berlin: Springer)
[32] Krapf D, Lukat N, Marinari E, Metzler R, Oshanin G, Selhuber-Unkel C, Squarcini A, Stadler L, Weiss M and Xu X 2019 *Phys. Rev.* X **9** 011019
[33] Beran J 1994 *Statistics for Long-Memory Processes* (New York: Chapman and Hall)
[34] Qian H 2003 *Processes with Long-Range Correlations: Theory and Applications* ed G Rangarajan and M Ding (Berlin: Springer)
[35] Redner S 2001 *A Guide to First Passage Processes* (Cambridge UK: Cambridge University Press)
     Metzler R and Klafter J 2000 *Physica* A **278** 107
[36] Ding M and Yang W 1995 *Phys. Rev.* E **52** 207
     Krug J, Kallabis H, Majumdar S N, Cornell S J, Bray A J and Sire C 1997 *Phys. Rev.* E **56** 2702
[37] Molchan G M 1999 *Commun. Math. Phys.* **205** 97
[38] Jeon J-H, Chechkin A V and Metzler R 2011 *Europhys. Lett.* **94** 20008
[39] Wiese K J, Majumdar S N and Rosso A 2011 *Phys. Rev.* E **83** 061141
[40] Deng W and Barkai E 2009 *Phys. Rev.* E **79** 011112
     Schwarzl M, Godec A and Metzler R 2017 *Sci Rep.* **7** 3878
[41] Kursawe J, Schulz J and Metzler R 2013 *Phys. Rev.* E **88** 062124
[42] Jeon J-H and Metzler R 2012 *Phys. Rev.* E **85** 021147
[43] Mura A and Pagnini G 2008 *J. Phys.* A **41** 285003
[44] Molina-García D, Pham T M, Paradisi P, Manzo C and Pagnini G 2016 *Phys. Rev.* E **94** 052147
[45] Lim S C and Muniandy S V 2002 *Phys. Rev.* E **66** 021114
     Jeon J-H, Chechkin A V and Metzler R 2014 *Phys. Chem. Chem. Phys.* **16** 15811
[46] Wada A H O and Vojta T 2018 *Phys. Rev.* E **97** 020102(R)
[47] Sliusarenko O, Gonchar V Y, Chechkin A V, Sokolov I M and Metzler R 2010 *Phys. Rev.* E **81** 041119
[48] Dieker T 2004 Simulation of fractional Brownian motion *Master Thesis* University of Twente, Enschede, The Netherlands
[49] Molina-Garcia D, Sandev T, Safdari H, Pagnini G, Chechkin A and Metzler R 2018 *New J. Phys.* **20** 103027
[50] Lampo T, Stylianido S, Backlund M P, Wiggins P A and Spakowitz A J 2017 *Biophys. J.* **112** 532
     Ślęzak J, Metzler R and Magdziarz M 2018 *New J. Phys.* **20** 023026
[51] Godec A, Bauer M and Metzler R 2014 *New J. Phys.* **16** 092002
[52] Kubo R 1966 *Rep. Prog. Phys.* **29** 255
     Hänggi P 1978 *Z. Phys.* B **31** 407
     Hänggi P and Mojtabai F 1982 *Phys. Rev.* E **26** 1168
     Kou S C 2008 *Ann. Appl. Stat.* **2** 501
     Kneller G 2014 *J. Chem Phys.* **141** 041105
[53] Goychuk I 2009 *Phys. Rev.* E **80** 046125
     Goychuk I 2012 *Adv. Chem. Phys.* **150** 187
[54] Chechkin A V, Klafter J, Yu V, Gonchar, Metzler R and Tanatarov L V 2003 *Phys. Rev.* E **67** 010102(R)